P9.5 Examining the Impact of Spatial and Temporal Resolutions of Phased-Array Radar on EnKF Analysis of Convective Storms Using OSSEs - Modeling Observation Errors

Y. Umemoto[1, 2], T. Lei[3], T. -Y. Yu[1, 2] and M. Xue[3, 4]

1: School of Electrical and Computer Engineering

2: Atmospheric Radar Research Center

3: Center for Analysis and Prediction of Storms

4: School of Meteorology

The University of Oklahoma, Norman, USA

1. INTRODUCTION

The S-band Phased Array Radar (PAR) at the National Weather Radar Testbed (NWRT) in Norman, Oklahoma can adaptively scan multiple regions of interest and provide rapidly updated weather observations by electronically beam steering. This capability allows providing fast updates of weather information with high statistical accuracy with scanning strategy termed beam multiplexing (Yu et al. 2007). Since PAR has wider beams (~2 degrees) than that of the operational WSR-88D (~1 degree), PAR has lower spatial resolutions at far ranges.

Among efforts to better realize its potential for improving convective-storm analysis and prediction, an EnKF system developed for the Advanced Regional Prediction System (ARPS) has recently been enhanced to use proper beam pattern and range weighting functions to assimilate radar data on a radial-by-radial basis. This capability allows us to take advantage of the range and azimuthal over-sampling capabilities of PAR data, and the ability for PAR to can gain better accuracy through beam multiplexing.

The earlier Observing System Simulation Experiments (OSSEs, e.g., Snyder et. al 2003; Zhang et. al 2004; Tong and Xue 2005, TX05 hereafter; Xue et. al 2006, TXD06 hereafter; Jung et. al 2008; Lei et. al 2007, L07 hereafter) have been extended to examine additional capabilities of the PAR in more realistic settings in this study. Confirming earlier results, azimuthal over-sampling and rapid update time are shown to improve the analysis. For these experiments, observation errors that are spatially inhomogeneous and scanning strategy-dependent are applied. By properly modeling the expected error in the observations for different scanning strategies, the results of the OSSEs become more robust.

This paper is organized as follows: in section 2, simulated radar data, the observational error models OSSEs experimental design and the specification of the ARPS EnKF system are described. Preliminary results are presented in section 3 and discussions are given in section 4.

2. ERROR MODELS AND EXPERIMENTAL DESIGN

2.1 EnKF system and simulated radar observation

In this experiment, the perfect model is assumed, and the same model and exactly the same configurations are used for the truth simulation and ensemble forecasts. The same observation operator is used in EnKF analysis and simulation of observation. The ARPS EnKF system used in this study is based on TX05, XTD06, and L07 including the ability to assimilate radar observations radial by radial in their native radar coordinates, which allows examining impact of various scanning strategies including over-sampling. Though the PAR has a range

* Corresponding author address: Yasuko Umemoto; 120 David L. Boren Blvd. Suite 5900, Norman, OK 73072, U.S.A.; E-mail: yasuko@ou.edu

resolution spacing of 250 m, simulated observations in this study has a range spacing that is no smaller than the grid interval of the truth simulation (1 km in horizontal).

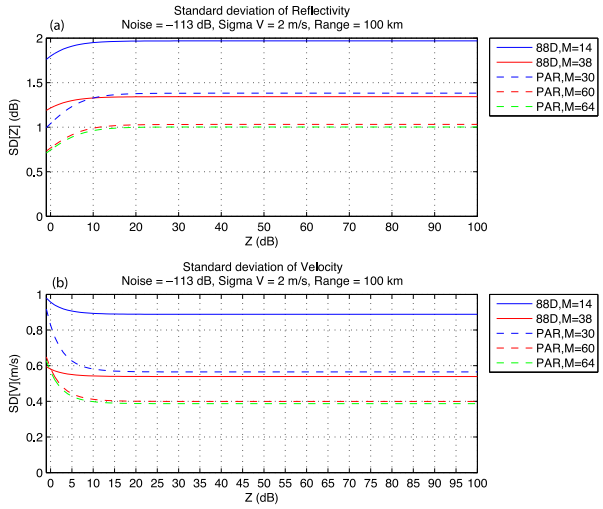

Fig. 1 SDs of reflectivity (top) and radial velocity (bottom) at 100 km from radars. The solid blue lines are for SDs for WSR-88d, M (number of pulse) = 14, the solid red lines are for WSR-88d, M = 38, the dashed blue lines are for PAR, M = 30, the dashed red lines are for PAR, M = 60, the dashed green lines are for PAR, M = 64.

2.2 Error models

For OSSEs, radar data with observational errors was typically simulated by adding random noise with a uniform standard deviation to the error-free observation that was estimated using the state variables from the output of numerical model. TX05 and XTD06 simulated reflectivity observation errors by adding noise to the simulated reflectivity that has a Gaussian distribution of zero mean and a standard deviation (SD) of 5 dBZ for all radar data L07 used SDs of 2 dBZ and 1 ms^{-1} for error estimation of reflectivity and radial velocity respectively. Although the reflectivity error is typically added in log domain, the error model has been extended to add error in a liner domain.

Two error models are examined in this study. For both error models, reflectivity error is added in liner domain. For the first, we assumed SD of Z is proportional to reflectivity and is written as follows:

$$SD[Z] = \alpha 10^{\frac{Z}{10}} \tag{1}$$

where α value of 38 % is found to yield effective error SD of 2.0 dBZ and Z is reflectivity. For this case, spatially homogeneous SD of radial velocity is assumed as 1 ms^{-1}. For the second model, the error estimation has been developed to be spatially inhomogeneous and scanning strategy-dependent. Specifically, the observation error is a function of the strength of radar return (signal to noise ratio, SNR), number of pulses, pulse repletion time, and distance from the radar (Doviak and Zarnic1993, Chapter 6). In this study, SNR is assumed as follows:

$$SNR = 10^{\left(\frac{Z-113}{10}\right)} \tag{2}$$

The uniform noise power with 113 dB is assumed in this study. From eq. (6.13) and (6.21) of Doviak and Zarnic 1993, SDs of reflectivity and radial velocity are written as follows:

$$SD[v] = \left[\lambda^2\left[32\pi^2 T_s^2 \rho^2(T_s)\right]^{-1}\left\{M^{-2}\left[1-\rho^2(T_s)\right]\right.\right.$$
$$\left.\sum_{m=-(M-1)}^{M-1}\rho^2(mT)(M-|m|)+\frac{1}{M}\frac{1}{SNR^2}\right. \tag{3}$$
$$\left.\left.+\frac{1}{M}\frac{2}{SNR}\left[1+\rho(2T_s)\left(\frac{1}{M}-1\right)\right]\right]^{\frac{1}{2}}$$

$$SD[Z] = Z\left\{\sum_{m=-(M-1)}^{M-1}\frac{M-|m|}{M^2}\right.$$

$$\left.\left\{\left(1+\frac{1}{SNR}\right)^{-1}\rho(mT_s)+(1+SNR)^{-1}\delta_{m,0}\right\}\right\}^{\frac{1}{2}} \quad (4)$$

where λ is wave length of radar, T_s and M are pulse repetition time and number of pulse of observation, respectively. $\rho(mT_s)$ is as follows:

$$\rho(mT_s) = \exp\left[-8(\pi\sigma_v mT_s/\lambda)^2\right] \quad \textbf{(5)}$$

σ_v is assumed to be 2 m/s in this study. Estimated SDs of reflectivity and radial velocity at 100 km from radars using above equations are shown in Fig. 1. As number of pulse increases, both SDs of reflectivity and radial velocity are decreased.

2.3 Experimental design

In this study, the 20 May Del City, Oklahoma supercell storm is simulated using ARPS to serve as the truth for OSSEs. The model domain is 64 x 64 x 20 km^3 with horizontal spacing of 1 km and 43 vertical levels. A thermal bubble placed at the low level of a horizontally homogeneous environment triggers the storm and the model is integrated for two hours. The main storm is located close to the domain at (32,32) km. The ensemble square root filter scheme is used in this study. Both reflectivity and radial velocity are assimilated from the first analysis cycle.

Table. 1 List of experiments.

Experiment	Radar	Beam width	Angular increment in athimuth/ elevation	Distance from the storm	Volume scan interval	Number of pulse	Effective error SD of Z (dBZ)	Effective Error SD of Vr (ms^{-1})
PF2a	PAR	2^o	2^o	130 km	2 min		2.0	1.0
PF1a	PAR	2^o	1^o	130 km	2 min		2.0	1.0
PF.5a	PAR	2^o	0.5^o	130 km	2 min		2.0	1.0
NF1a	NEXRAD	1^o	1^o	130 km	2 min		2.0	1.0
PS2a64	PAR	2^o	2^o	130 km	5 min	64	0.82	1.04
PS1a64	PAR	2^o	1^o	130 km	5 min	64	0.81	1.04
PS.5a64	PAR	2^o	0.5^o	130 km	5 min	64	0.81	1.05
NS1a38	NEXRAD	1^o	1^o	130 km	5 min	38	1.48	0.72
PS2b64	PAR	2^o	2^o	30 km	5 min	64	1.14	0.42
PS1b64	PAR	2^o	1^o	30 km	5 min	64	1.14	0.42
PS.5b64	PAR	2^o	0.5^o	30 km	5 min	64	1.15	0.42
NS1b38	NEXRAD	1^o	1^o	30 km	5 min	38	1.92	0.54
PF2a64	PAR	2^o	2^o	130 km	2 min	64	0.81	1.04
PF1a60	PAR	2^o	1^o	130 km	2 min	60	0.83	1.05
PF.5a30	PAR	2^o	0.5^o	130 km	2 min	30	1.28	1.48
NF1a14	NEXRAD	1^o	1^o	130 km	2 min	14	2.6	1.15

Though all radial velocity observations are used in the analysis, reflectivity observations less than 5 dBZ are not used. The initial ensemble forecast starts at 20 min of model time. The initial ensembles are specified by adding smoothed random perturbations to the initial guess defined by the truth simulation sounding as in TX05, XTD06 and L07. We designed 16 experiments as listed in Table 1. In the experiment names, P and N stands for "Assimilation of PAR radar data and NEXRAD (WSR-88d), respectively". S and F in the names denote "Slow (5min) and Fast (2min) volume scan interval, respectively". The following number, 2, 1, .5 denote angular increment in athimuth / elevation. "a" and "b" stand for experiments in which radar is located at (-100,0) km and (0,0) km southwest corner of the model domain. The last two-digit number represents the assumed number of pulse.

3. RESULT

As shown in Table 1, in PS2a64, observational error is estimated with equations mentioned before for number of pulse = 64. For this case, Effective errors SDs of 0.8 dBZ and 1.04 ms^{-1} are yield when numerically calculated for Z and Vr data at all data assimilation times, respectively. It is assumed that PAR and WSR-88D have the beam width of 2^o and 1^o, respectively. It is shown in (a) that PAR oversampling with 1 or 0.5 degrees increment (PS1a64 or PS.5a64) show better performance than WSR-88D that has 1 degree beam width without oversampling (NS1a38), when the storm is located far from the radar and data is assimilated every 5 minutes. On the other hand, if the storm is located close to the radar, the improvement provided by oversampling is not obvious, as shown in (b). For this case, conventional scanning using WSR-88D (NS1b38) shows the best performance. It suggests that the PAR should mimic the WSR-88D's scanning pattern for this case. When radar data assimilated in a shorter cycle (every 2 minutes), RMS errors are reduced much more rapidly than the one with longer cycle as shown in (c). However, the RMS errors reach the lower limit faster if the storm is located far from radar. Generally speaking, observations with fast updates can be achieved using fewer sampling, which leads to the degradation of data accuracy. However, PAR can adaptively scan multiple regions of interest and provide rapidly updated observation by electronically beam steering. This capability allows fast updates of weather information without comprising data accuracy. When the scanning strategies are taken into account for error estimation, conventional scanning pattern by WSR-88D shows worse result than PAR oversampling as shown in (c). On the other hand, WSR-88D's scanning pattern shows as good performance as PAR oversampling as shown in (d) when the error is scanning strategy independent.

3. DISCUSSION

The impact of scanning strategies including oversampling was re-examined using the more realistic error model. When the scanning strategies are taken into account for error estimation, conventional scanning pattern by WSR-88D shows worse result than PAR oversampling. On the other hand, WSR-88D's scanning pattern shows as good performance as PAR oversampling when the error is scanning strategy independent. By properly modeling the expected error in the observations for different scanning strategies, the results of the OSSEs become more robust.

Acknowledgement This work is supported by ONR DEPSCOR Program grant DOD-ONR N00014-06-1-0590.

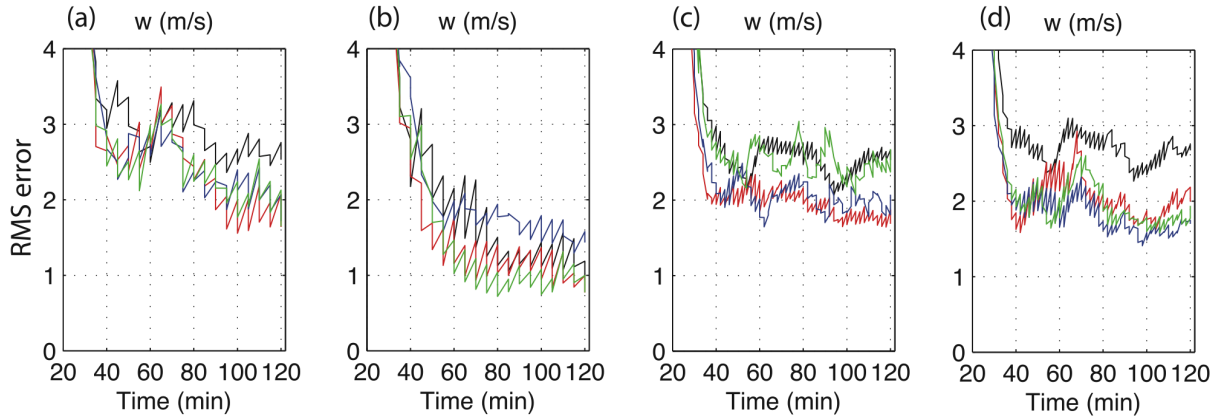

Fig. 2 Ensemble-mean forecast and analysis of RMS errors for vertical velocity w. PS2a64 (black), PS1a64 (blue), PS.5a64 (red) and NS1a38 (green) are shown in (a). PS2b64 (black), PS1b64 (blue), PS.5b64 (red) and NS1b38 (green) are shown in (b). PF2a64 (black), PF1a60 (blue), PF.5a30 (red) and NF1a14 (green) are shown in (c). PS2a (black), PS1a (blue), PS.5a (red) and NS1a (green) are shown in (d).

Reference:

Doviak, R., and D. Zarnic, 1993: Doppler Radar and Weather Observations, *2nd ed., Elsevier, NowYork.*

Jung, Y., M. Xue, G. Zhang, and J. Straka, 2008: Assimilation of simulated polarimetric radar data for a convective storm using ensemble Kalman filter. Part II: Impact of polarimetric data on storm analysis. *Mon. Weather Rev.*, **136**, 1649--1668.

Lei, T., M. Xue, T.-Y. Yu, and M. Teshiba, 2007: Study on the optimal scanning strategies of phased-array radar through ensemble Kalman filter ssimilation of simulated data. *33rd Int. Conf. Radar Meteor.,Cairns, Australia,* P7.1.

Snyder, C, and F. Zhang, 2003: Assimilation of simulated Doppler radar observations with an ensemble Kalman filter. *Mon. Weather Rev.*, **131**, 1663--1677.

Tong, M., and M. Xue, 2005: Ensemble Kalman filter assimilation of Doppler radar data with a compressible nonhydrostatic model: OSSE Experiments. *Mon. Weather Rev.,* **133**, 1789--1807.

Xue, M., M. Tong, and K. K. Droegemeier, 2006: An OSSE framework based on the ensemble squareroot Kalman filter for evaluating impact of data from radar networks on thunderstrom analysis and forecast. *J. Atmos. Oceanic Technol.*, **23**, 46--66.

Yu, T.-Y., M. B. Orescanin, C ~D. Curtis, D. S. Zrnic, and D. E. Forsyth, 2007: Beam multiplexing using the pahsed-array weather radar. *J. Atmos. Oceanic Technol.*, **24**, 103--118.

Zhang, F., C. Snyder, and J. Sun, 2004: Impacts of initial estimate and observations on the convective-scale data assimilation with an ensemble Kalman filter. *Mon. Weather Rev.*, **132**, 1238—125.